Nanotechnology

International Edition: DOI: 10.1002/anie.201604980
German Edition: DOI: 10.1002/ange.201604980

Organic-Stabilizer-Free Polyol Synthesis of Silver Nanowires for Electrode Applications

*Hwansu Sim[+], Shingyu Bok[+], Bongsung Kim, Minha Kim, Guh-Hwan Lim, Sung Min Cho, and Byungkwon Lim**

Abstract: *The polyol reduction of a Ag precursor in the presence of an organic stabilizer, such as poly(vinylpyrrolidone), is a widely used method for the production of Ag nanowires (NWs). However, organic capping molecules introduce insulating layers around each NW. Herein we demonstrate that Ag NWs can be produced in high yield without any organic stabilizers simply by introducing trace amounts of NaCl and $Fe(NO_3)_3$ during low-temperature polyol synthesis. The heterogeneous nucleation and growth of Ag NWs on initially formed AgCl particles, combined with oxidative etching of unwanted Ag nanoparticles, resulted in the selective formation of long NWs with an average length of about 40 μm in the absence of a capping or stabilizing effect provided by surface-adsorbing molecules. These organic-stabilizer-free Ag NWs were directly used for the fabrication of high-performance transparent or stretchable electrodes without a complicated process for the removal of capping molecules from the NW surface.*

Silver nanowires (NWs) have attracted great interest owing to their high electrical conductivity, solution processability, and potential for applications in highly conductive transparent or stretchable electrodes.[1–3] During the last decade, there has been considerable effort to develop an effective strategy for the reliable and scalable production of Ag NWs in high yield.[4] The polyol reduction of $AgNO_3$ in the presence of poly(vinylpyrrolidone) (PVP) has been the most widely used method for the production of Ag NWs, whereby PVP has long been considered to be necessary to promote NW formation because of its role in stabilizing the {100} side faces of growing NWs.[5] However, these long-chain polymeric molecules introduce insulating layers around each NW, thus dramatically increasing contact resistance between NWs in electrode applications.[6] A typical procedure for removing organic capping layers from the NW surface involves many cycles of the precipitation and redispersion of NWs in a good solvent for capping molecules, which is tedious and time-consuming.[7] Despite considerable progress in NW synthesis, the production of Ag NWs for electrode applications still relies on a PVP-mediated polyol method, and the organic-stabilizer-free, high-yielding synthesis of Ag NWs remains a great challenge.

Herein we report a modified polyol synthesis of Ag NWs and demonstrate that it is possible to produce NWs in high yield without the use of any organic stabilizers. Our synthesis is simple and only involves the use of ethylene glycol (EG), $AgNO_3$, and trace amounts of NaCl and $Fe(NO_3)_3$. We found that AgCl particles, which were initially formed from the reaction of some of the $AgNO_3$ and NaCl, provided preferential sites for the heterogeneous nucleation and growth of Ag NWs, thus allowing selective NW formation without the aid of a capping or stabilizing effect provided by surface-adsorbing molecules. By using this simple approach, we were able to produce long Ag NWs with a length of approximately 40 μm and a diameter of approximately 45 nm on average in high yield. These Ag NWs were successfully used for the fabrication of transparent electrodes, whose performance was comparable to that of electrodes made of indium tin oxide (ITO), as well as stretchable electrodes. Our synthetic strategy provides an efficient route for the fabrication of high-performance transparent or stretchable electrodes based on Ag NWs because it does not require an additional process for the removal of capping molecules from the NW surface.

In this study, Ag NWs were synthesized by the heating of an EG solution containing $AgNO_3$ (150 μmol) and trace amounts of NaCl (0.9 μmol) and $Fe(NO_3)_3$ (6 μmol) at 110 °C for 15 h without stirring. A series of color changes occurred during the synthesis (see Figure S1 in the Supporting Information). Scanning electron microscopy (SEM) analysis of the product revealed the formation of Ag NWs in high yield (ca. 91 %; Figure 1 A; see also Figure S2). The resulting NWs had an average diameter of about 45 nm and an average length of about 40 μm (Figure 1 B; see also Figures S3 and S4). The NWs had a pentagonal cross-section (Figure 1 B, inset), thus indicating that they were grown from fivefold twinned seeds. Figure 1 C shows a typical transmission electron microscopy (TEM) image of a single NW. The corresponding electron diffraction (ED) pattern consisting of more than one set of spots is indicative of its twinned structure (Figure 1 C, inset). The product contained very few Ag NPs (ca. 9 %; see Figures S2 and S5). In the powder X-ray diffraction (XRD) pattern taken from the product (Figure 1 D), the diffraction peaks at 2θ values of 38.1, 44.3, 64.5, and 77.4° could be

[*] H. Sim,[+] S. Bok,[+] G.-H. Lim, Prof. B. Lim
School of Advanced Materials Science and Engineering
Sungkyunkwan University (SKKU)
Suwon 16419 (Korea)
E-mail: blim@skku.edu

B. Kim, M. Kim
SKKU Advanced Institute of Nanotechnology (SAINT)
Sungkyunkwan University (SKKU)
Suwon 16419 (Korea)

Prof. S. M. Cho
School of Chemical Engineering, Sungkyunkwan University (SKKU)
Suwon 16419 (Korea)

[+] These authors contributed equally.

Supporting information for this article can be found under: http://dx.doi.org/10.1002/anie.201604980.

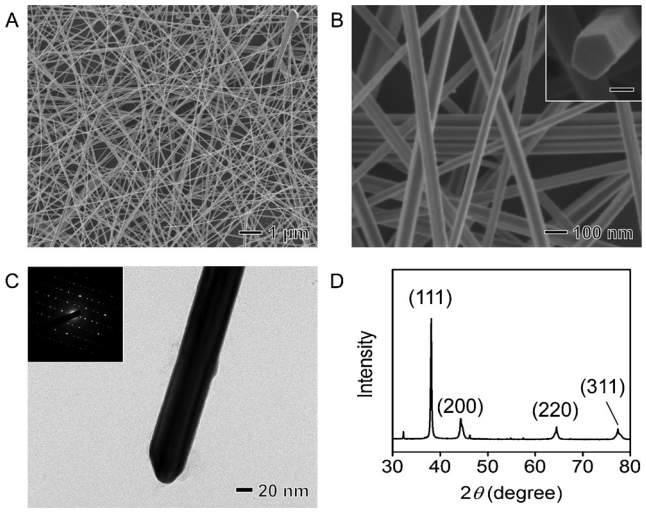

Figure 1. A, B) SEM images of as-synthesized Ag NWs. The inset in (B) shows the pentagonal cross-section of a single NW. The scale bar in the inset is 50 nm. C) TEM image of a single Ag NW and the corresponding ED pattern (inset). D) Powder XRD pattern of the product shown in (A).

indexed to (111), (200), (220), and (311) reflections of face-centered-cubic (fcc) Ag (JCPDS Card No. 04-0783), respectively.

We monitored the growth process of Ag NWs by UV/Vis spectroscopy and electron microscopy (Figure 2). The UV/Vis spectra recorded at different stages of the synthesis are shown in Figure 2A. Until 7 h, no characteristic peaks associated with Ag NWs appeared in the UV/Vis spectrum. SEM analysis of the sample taken at $t = 3$ h revealed that it mainly contained AgCl particles (Figures 2B; see also Figure S6). The UV/Vis spectrum recorded at $t = 8$ h showed the appearance of two peaks centered at 355 and 385 nm. The latter is associated with the transverse plasmon resonance of Ag NWs, thus indicating that NW growth had begun to occur. The sample taken at this stage contained a number of nanorods and NWs branching out from AgCl cores (Figure 2C, D). The surface of AgCl particles was also decorated with Ag nanoparticles (NPs), as revealed by high-angle annular dark-field scanning TEM (HAADF-STEM) and energy-dispersive X-ray spectroscopy (EDS) line scanning analyses (Figure 3A, B). As the synthesis proceeded, NWs grew further in length, whereas the number of particles decreased dramatically, leaving behind long Ag NWs in high yield (Figure 2E, F). These observations indicate that NW growth occurred by the heterogeneous nucleation of Ag on initially formed AgCl particles.

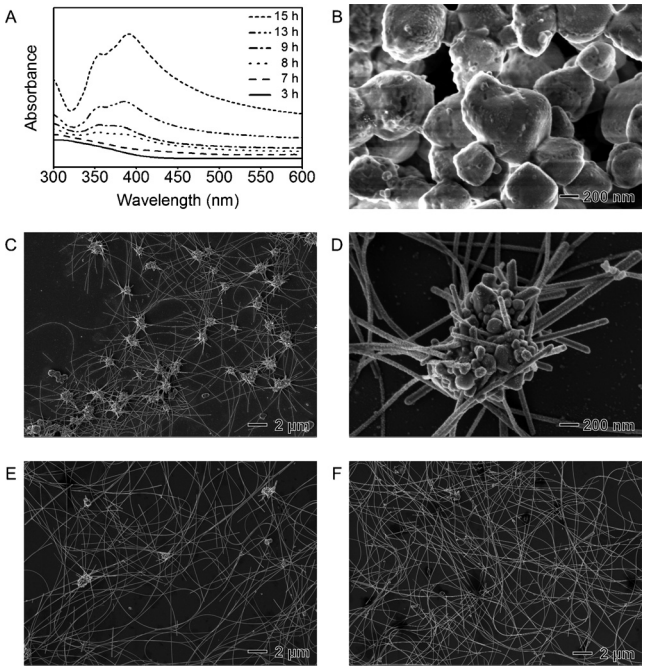

Figure 2. A) UV/Vis spectra recorded at different stages of the synthesis. B–F) SEM images of samples taken at different stages of the synthesis: 3 h (B), 8 h (C, D), 11 h (E), and 13 h (F).

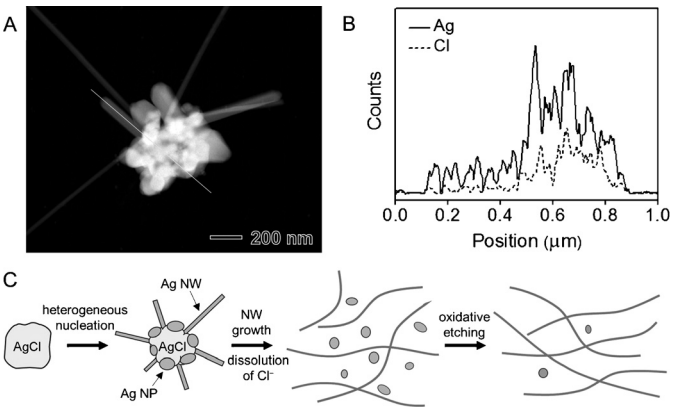

Figure 3. A) HAADF-STEM image of Ag NWs and NPs grown from a AgCl core (recorded for a sample taken at 8 h). B) Compositional line profiles of Ag and Cl recorded along the line shown in (A). C) Proposed nucleation and growth mechanism of Ag NWs.

The selective formation of Ag NWs in the absence of any organic stabilizers is intriguing. At early stages of this synthesis, some of the $AgNO_3$ and NaCl reacted to form AgCl particles, which serve as heterogeneous nucleants for Ag (Figure 3C). At the nucleation stage, seeds can take a decahedral shape in an attempt to minimize the total free energy by maximizing the surface coverage with low-energy {111} facets. Once Ag has nucleated on the AgCl surface, which provides multiple nucleation sites, Ag nuclei can grow into either NPs or NWs rather than a continuous overlayer owing to a large lattice mismatch between Ag and AgCl (ca. 26.4% mismatch). One-dimensional growth of NWs in an outward direction from a AgCl core may occur without a significant increase in lattice strain energy that might otherwise be caused by the lattice mismatch at the interface between Ag and AgCl as well as internal twin defects, and thus would be more favorable than the quasi-isotropic growth of NPs. During the growth stage, Ag cations in AgCl may be reduced to metallic Ag by EG and incorporated into growing NWs or NPs, while Cl anions are dissolved into the solution. At later stages of the synthesis, the number of Ag NPs

dramatically decreases to leave behind NWs in high yield, which might be attributed to the oxidative etching of NPs by O_2/Cl^- pairs.[8] As a control experiment, we conducted the synthesis in the absence of chloride ions. In this case, the product mainly contained irregular Ag particles as well as a small portion of short NWs with a broad range of thicknesses (see Figure S7), thus indicating loss of selectivity for NW formation. In the absence of O_2/Cl^- pairs, twinned seeds formed by homogeneous nucleation in solution can survive and grow into large particles as well. Although AgCl-mediated polyol syntheses of Ag NWs have been reported previously,[9] the previous syntheses still involved the use of PVP. Our results clearly show that selective NW formation is possible by AgCl-mediated synthesis that does not involve the use of any organic stabilizers as structure-directing agents. Ag nanostructures did not form in the absence of Fe ions (see Figure S8), which seem to play a role in facilitating the reduction of Ag ions by EG at a relatively low temperature, as suggested by a previous study by the Xia group.[10] The EDS line scanning analysis of a growing NW also revealed the presence of Cl ions adsorbed on the surface of the NW (Figure 3A,B). It seems that the surface-adsorbed Cl ions play a role in stabilizing Ag NWs by causing electrostatic repulsion between the NWs.

We tested our Ag NWs for application in transparent electrodes. To prepare the NW dispersion for the coating of a substrate, the as-synthesized NWs in EG were transferred to isopropyl alcohol (IPA) with only two cycles of precipitation and redispersion of NWs (see Figure S9). The EDS analysis of a Ag NW film prepared on a Si substrate revealed the presence of residual organic species on the surface of Ag NWs (see Figure S10). It is thought that some EG may remain on the surface of our Ag NWs after the solvent exchange and subsequent drying process. For the fabrication of transparent electrodes, Ag NWs were deposited onto a poly(ethylene terephthalate) (PET) substrate by a bar-coating method with a Meyer rod. After coating, the substrate was immersed in an aqueous NaCl solution (10 wt%) at room temperature for 40 s and then washed with water. This simple salt treatment was shown to effectively induce welding at junctions of NWs.[7c] Figure 4A shows an SEM image of a Ag NW network film on a PET substrate prepared by bar coating and subsequent salt treatment. It can be seen that the NWs are evenly distributed on the substrate without aggregation. Figure 4B shows a plot of transmittance at a wavelength of 550 nm versus sheet resistance for Ag NW films with different NW densities. The Ag NW film exhibited a transmittance of 94.8% at 40.2 Ω/sq, which is comparable to the performance of ITO (transmittance of 95% at 50 Ω/sq) and much better than that of PVP-stabilized Ag NWs (see Figure S11). Hence, our organic-stabilizer-free synthesis of Ag NWs offers an efficient strategy for the fabrication of highly conductive, transparent, and flexible electrodes without the need for a complicated procedure for the removal of organic capping molecules from the NW surface.

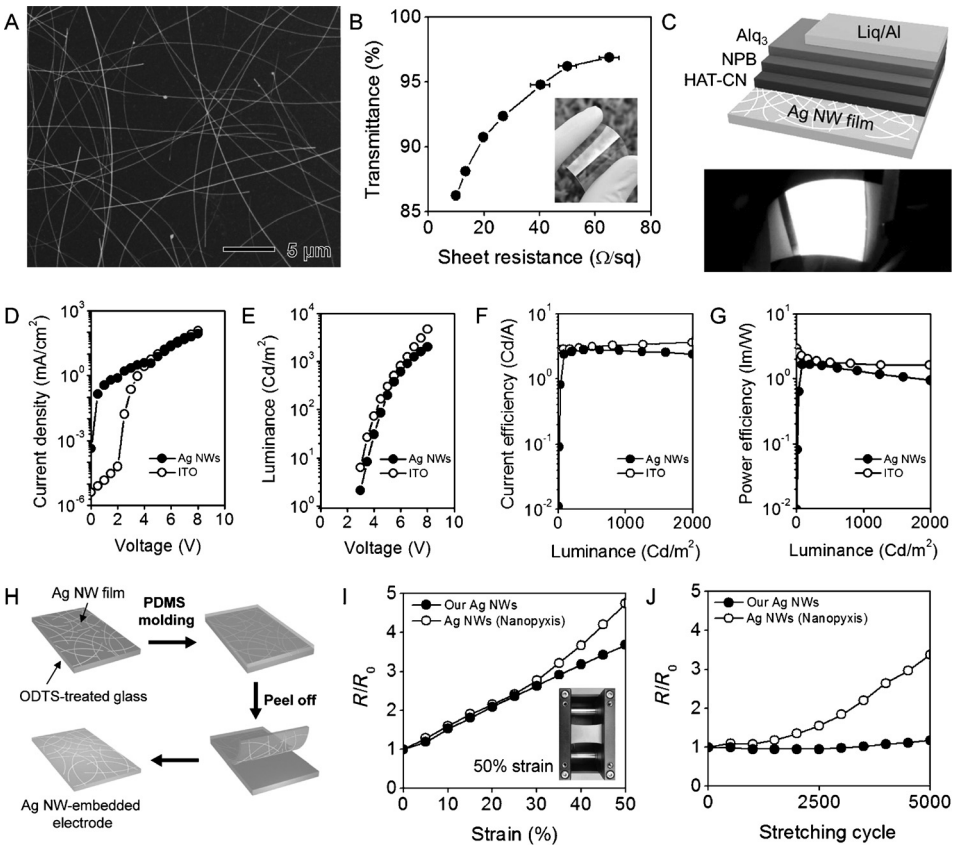

Figure 4. A) SEM image of a Ag NW film prepared on a PET substrate by bar coating of the NW dispersion in IPA. B) Plot of transmittance at a wavelength of 550 nm versus sheet resistance for Ag NW electrodes with different NW densities. The inset shows an optical image of a Ag NW transparent electrode under bending. C) Schematic diagram of an OLED based on an Ag NW anode (Alq_3 = tri(8-hydroxyquinolinato)aluminum, HAT-CN = 1,4,5,8,9,11-hexaazatriphenylene-hexacarbonitrile, NPB = *N,N′*-bis-(1-naphthyl)-*N,N′*-diphenyl-1,1′-biphenyl-4,4′-diamine). A light-emission image of the OLED under bending is also shown. D, E) Current-density–voltage–luminance characteristics of OLEDs based on the Ag NWs and ITO. F, G) Current efficiency and power efficiency as a function of the luminance of OLEDs based on the Ag NWs and ITO. H) Fabrication process of the silver-nanowire-embedded stretchable electrodes (ODTS = octadecyltrichlorosilane). I) Change in resistance (R/R_0) for silver-nanowire-embedded stretchable electrodes in response to tensile strain. The inset shows an optical image of an electrode prepared with our Ag NWs under stretching at 50% strain. J) Variation in the change in resistance (R/R_0) for the silver-nanowire-embedded electrodes during 5000 cycles of stretching at 30% strain. During the cycles, the resistance was measured after release of the strain.

The transparent Ag NW film was successfully used in an organic light-emitting diode (OLED) device. Figure 4C shows the basic structure of our OLED based on Ag NWs. Figure 4D,E shows the current-density–voltage–luminance characteristics of the OLED prepared with the Ag NW electrode in comparison with those of a reference OLED prepared with commercial ITO. The OLED prepared with our Ag NWs showed a higher current density than the ITO-based OLED at low voltages below 4 V as result of the higher leakage current originating from the higher surface roughness of the Ag NW film as compared to that of ITO. At high voltages beyond 4 V, the current density and luminance of the silver-nanowire-based OLED were comparable to those of the ITO-based OLED. The luminous current and power efficiencies of the silver-nanowire-based OLED were also comparable (2.7 $Cd\,A^{-1}$ and 1.3 $lm\,W^{-1}$ at 1000 $Cd\,m^{-2}$) to the corresponding values for the ITO-based OLED (3.3 $Cd\,A^{-1}$ and 1.7 $lm\,W^{-1}$ at 1000 $Cd\,m^{-2}$; Figure 4F,G). These results suggest that our transparent electrodes based on Ag NWs are promising alternatives to brittle ITO electrodes and thus for the preparation of flexible displays.

We also fabricated a highly stretchable and durable electrode by embedding a Ag NW network film in a polydimethylsiloxane (PDMS) elastomer (Figure 4H). This embedded Ag NW electrode exhibited high stability in a 3M Scotch tape detachment test, with its resistance remaining constant during 100 detachment cycles (see Figure S12). For comparison, an electrode was also prepared by the same protocol except for the use of commercially available Ag NWs (Nanopyxis), which were 20 μm in length on average (see Figure S13). Figure 4I shows plots of the change in resistance with tensile strain for the two electrodes. Both exhibited similar behavior up to 30% strain, with the R/R_0 value increasing with strain, where R and R_0 are the resistance measured at a given strain and initially, respectively. At large strains (>30%), the electrode prepared with our Ag NWs showed slightly better performance than that prepared with the commercial Ag NWs. The resistance of the electrode prepared with our Ag NWs remained nearly unchanged during stretching/releasing cycles (5000 cycles) at a tensile strain of 30% (Figure 4J); the resistance was measured after the strain was released, thus demonstrating the excellent electrical stability of the electrode. However, the resistance of the electrode prepared from the commercial Ag NWs with relatively short lengths increased continuously during repeated stretching/release cycles at the same strain. The stretchable electrode fabricated with our Ag NWs is characterized by a percolating network consisting of long NWs with an average length of approximately 40 μm, which would be beneficial in maintaining electrical contacts between NWs and recovering the original percolating network during stretching/release cycles.[11]

In summary, we have demonstrated a high-yielding polyol synthesis of Ag NWs without the use of any organic stabilizers. Our results clearly show that by exploiting the heterogeneous nucleation and growth of Ag in the presence of AgCl nucleants, it is possible to achieve high selectivity for NW formation even in the absence of a capping effect provided by organic stabilizers. We have also shown that these organic-stabilizer-free Ag NWs could be directly applied to the fabrication of high-performance transparent or stretchable electrodes without the need for a surface-decapping process.

Acknowledgments

This research was supported by the Center for Advanced Soft Electronics (CASE) under the Global Frontier Research Program (2013M3A6A5073177) by the Ministry of Science, ICT and Future Planning, and by the Information Technology Research Center (ITRC) under the support program (IITP-2016-H8501-16-1009) supervised by the Institute for Information and Communications Technology Promotion (IITP).

Keywords: nanotechnology · nanowires · nucleation · silver · transparent electrodes

How to cite: *Angew. Chem. Int. Ed.* **2016**, *55*, 11814–11818
Angew. Chem. **2016**, *128*, 11993–11997

[1] a) S. De, T. M. Higgins, P. E. Lyons, E. M. Doherty, P. N. Nirmalraj, W. J. Blau, J. J. Boland, J. N. Coleman, *ACS Nano* **2009**, *3*, 1767–1774; b) L. Hu, H. S. Kim, J.-Y. Lee, P. Peumans, Y. Cui, *ACS Nano* **2010**, *4*, 2955–2963; c) V. Scardaci, R. Coull, P. E. Lyons, D. Rickard, J. N. Coleman, *Small* **2011**, *7*, 2621–2628; d) T. Tokuno, M. Nogi, M. Karakawa, J. Jiu, T. T. Nge, Y. Aso, K. Suganuma, *Nano Res.* **2011**, *4*, 1215–1222; e) R. Zhu, C.-H. Chung, K. C. Cha, W. Yang, Y. B. Zheng, H. Zhou, T.-B. Song, C.-C. Chen, P. S. Weiss, G. Li, Y. Yang, *ACS Nano* **2011**, *5*, 9877–9882; f) A. Kim, Y. Won, K. Woo, C.-H. Kim, J. Moon, *ACS Nano* **2013**, *7*, 1081–1091; g) H. Lu, D. Zhang, X. Ren, J. Liu, W. C. H. Choy, *ACS Nano* **2014**, *8*, 10980–10987; h) H.-G. Cheong, J.-H. Kim, J.-H. Song, U. Jeong, J.-W. Park, *Thin Solid Films* **2015**, *589*, 633–641.

[2] a) X.-Y. Zeng, Q.-K. Zhang, R.-M. Yu, C.-Z. Lu, *Adv. Mater.* **2010**, *22*, 4484–4488; b) W. Gaynor, G. F. Burkhard, M. D. McGehee, P. Peumans, *Adv. Mater.* **2011**, *23*, 2905–2910; c) Z. Yu, Q. Zhang, L. Li, Q. Chen, X. Niu, J. Liu, Q. Pei, *Adv. Mater.* **2011**, *23*, 664–668.

[3] a) F. Xu, Y. Zhu, *Adv. Mater.* **2012**, *24*, 5117–5122; b) J. Ge, H.-B. Yao, X. Wang, Y.-D. Ye, J.-L. Wang, Z.-Y. Wu, J.-W. Liu, F.-J. Fan, H.-L. Gao, C.-L. Zhang, S.-H. Yu, *Angew. Chem. Int. Ed.* **2013**, *52*, 1654–1659; *Angew. Chem.* **2013**, *125*, 1698–1703; c) H.-L. Gao, L. Xu, F. Long, Z. Pan, Y.-X. Du, Y. Lu, J. Ge, S.-H. Yu, *Angew. Chem. Int. Ed.* **2014**, *53*, 4561–4566; *Angew. Chem.* **2014**, *126*, 4649–4654.

[4] a) J.-Q. Hu, Q. Chen, Z.-X. Xie, G.-B. Han, R.-H. Wang, B. Ren, Y. Zhang, Z.-L. Yang, Z.-Q. Tian, *Adv. Funct. Mater.* **2004**, *14*, 183–189; b) D. Zhang, L. Qi, J. Yang, J. Ma, H. Cheng, L. Huang, *Chem. Mater.* **2004**, *16*, 872–876; c) Z. Wang, J. Liu, X. Chen, J. Wan, Y. Qian, *Chem. Eur. J.* **2005**, *11*, 160–163; d) C. Yang, H. Gu, W. Lin, M. M. Yuen, C. P. Wong, M. Xiong, B. Gao, *Adv. Mater.* **2011**, *23*, 3052–3056.

[5] a) Y. Sun, B. Gates, B. Mayers, Y. Xia, *Nano Lett.* **2002**, *2*, 165–168; b) Y. Sun, Y. Xia, *Adv. Mater.* **2002**, *14*, 833–837; c) Y. Sun, B. Mayers, T. Herricks, Y. Xia, *Nano Lett.* **2003**, *3*, 955–960; d) B. Wiley, Y. Sun, Y. Xia, *Langmuir* **2005**, *21*, 8077–8080; e) W. A. Al-Saidi, H. Feng, K. A. Fichthorn, *Nano Lett.* **2012**, *12*, 997–1001; f) W. A. Saidi, H. Feng, K. A. Fichthorn, *J. Phys. Chem. C* **2013**, *117*, 1163–1171; g) G.-H. Lim, S. J. Lee, I. Han, S. Bok, J. H. Lee, J. Nam, J. H. Cho, B. Lim, *Chem. Phys. Lett.* **2014**, *602*,

10 – 15; h) B. Li, S. Ye, I. E. Stewart, S. Alvarez, B. J. Wiley, *Nano Lett.* **2015**, *15*, 6722 – 6726.
[6] a) J.-Y. Lee, S. T. Connor, Y. Cui, P. Peumans, *Nano Lett.* **2008**, *8*, 689 – 692; b) E. C. Garnett, W. Cai, J. J. Cha, F. Mahmood, S. T. Connor, M. G. Christoforo, Y. Cui, M. D. McGehee, M. L. Brongersma, *Nat. Mater.* **2012**, *11*, 241 – 249; c) P. Lee, J. Lee, H. Lee, J. Yeo, S. Hong, K. H. Nam, D. Lee, S. S. Lee, S. H. Ko, *Adv. Mater.* **2012**, *24*, 3326 – 3332.
[7] a) J.-Y. Lee, S. T. Connor, Y. Cui, P. Peumans, *Nano Lett.* **2010**, *10*, 1276 – 1279; b) T. Kim, Y. W. Kim, H. S. Lee, H. Kim, W. S. Yang, K. S. Suh, *Adv. Funct. Mater.* **2013**, *23*, 1250 – 1255; c) S. J. Lee, Y.-H. Kim, J. K. Kim, H. Baik, J. H. Park, J. Lee, J. Nam, J. H. Park, T.-W. Lee, G.-R. Yi, J. H. Cho, *Nanoscale* **2014**, *6*, 11828 – 11834.
[8] a) Y. Xiong, J. Chen, B. Wiley, Y. Xia, *J. Am. Chem. Soc.* **2005**, *127*, 7332 – 7333; b) K. E. Korte, S. E. Skrabalak, Y. Xia, *J. Mater. Chem.* **2008**, *18*, 437 – 441.
[9] a) W. M. Schuette, W. E. Buhro, *ACS Nano* **2013**, *7*, 3844 – 3853; b) W. M. Schuette, W. E. Buhro, *Chem. Mater.* **2014**, *26*, 6410 – 6417.
[10] S. E. Skrabalak, B. J. Wiley, M. Kim, E. V. Formo, Y. Xia, *Nano Lett.* **2008**, *8*, 2077 – 2081.
[11] M. Amjadi, A. Pichitpajongkit, S. Lee, S. Ryu, I. Park, *ACS Nano* **2014**, *8*, 5154 – 5163.

Received: May 20, 2016
Published online: August 29, 2016

